Adequacy of damped dynamics to represent the electron-phonon interaction in solids

A. Caro,[1,*] A. A. Correa,[2] A. Tamm,[1] G. D. Samolyuk,[3] and G. M. Stocks[3]

[1]*Materials Science and Technology Division, Los Alamos National Laboratory, Los Alamos, New Mexico 87545, USA*

[2]*Quantum Simulations Group, Lawrence Livermore National Laboratory, Livermore, California 94550, USA*

[3]*Materials Science and Technology Division, Oak Ridge National Laboratory, Oak Ridge, Tennessee 54321, USA*

(Received 3 June 2015; revised manuscript received 1 September 2015; published 16 October 2015)

Time-dependent density functional theory and Ehrenfest dynamics are used to calculate the electronic excitations produced by a moving Ni ion in a Ni crystal in the case of energetic MeV range (electronic stopping power regime), as well as thermal energy meV range (electron-phonon interaction regime). Results at high energy compare well to experimental databases of stopping power, and at low energy the electron-phonon interaction strength determined in this way is very similar to the linear response calculation and experimental measurements. This approach to electron-phonon interaction as an electronic stopping process provides the basis for a unified framework to perform classical molecular dynamics of ion-solid interaction with *ab initio* type nonadiabatic terms in a wide range of energies.

DOI: 10.1103/PhysRevB.92.144309 PACS number(s): 79.20.Rf, 79.20.Ap, 81.40.Wx, 83.10.Mj

I. INTRODUCTION

The Born-Oppenheimer approximation (BOA) [1] is the keystone to describe ionic motion in condensed matter. This approximation, in which ions move classically under the forces derived from the electronic ground-state energy, proved to be useful to describe nuclear stopping power for low-energy ions in solids, S_n. However, for ion energies approaching the Fermi velocity of electrons in the target, electronic loses, or nonadiabatic effects, become increasingly relevant. The rate of energy transfer to electrons can be cast in the form of an electronic stopping power S_e that, together with S_n, are the two mechanisms of energy dissipation for energetic ions colliding with a target material. As part of the BOA, S_n and S_e are customarily assumed to be independent of each other; however, in the presence of nonadiabatic energy exchanges, actual materials' response is beyond the BOA.

For projectile velocities below the target Fermi velocity, S_n and S_e are both relevant, creating a complex nonequilibrium situation that can be studied with a diversity of theoretical approaches. To a large extent, computational studies of radiation damage have ignored the dynamic response of the electrons to such perturbation; the majority has been done within the BOA, or with classical potentials, ignoring electron dynamics. From the early days, authors noticed the necessity to go beyond this approximation, ranging from collision cascades [2–11] and rapid shocks [12] to current-induced forces [13].

In addition to the phenomena related to stopping power (S_n and S_e), the electron-phonon (e-ph) interaction is also important, since it is responsible for the return to thermal equilibrium between the nuclear and electronic subsystems. In this work the expression electron-phonon interaction refers to both, the interaction of electrons with well-defined collective ionic motion excitations characterized by wave and polarization vectors, and the local picture of ions moving individually. Hybrid models combine different aspects of the problem in an *ad hoc* manner; these include two-temperature models (TTM) [2,3], phenomenological stopping based in the local density [4], collective excitations in a Coulomb explosion [5–8], and thermal spike approaches [2,3,9,10]. In general, these approaches consider a classical "electronic thermal" field evolving via heat transport equations, and coupled to ions via Langevin dynamics [11].

In the state-of-the-art implementations of classical molecular dynamics (MD) with two temperatures, such as Duffy's [11,14–16], a viscous damping term (βv) and a random force (ξ) are added to the Newton equations of motion of each ion: $F = -\beta v + \xi(t)$, where β is a piecewise function known in two limits: (i) $\beta = \beta_{S_e} + \beta_{\text{e-ph}}$ for $v_0 < v < v_F$ and (ii) $\beta = \beta_{\text{e-ph}}$ for $v < v_0$ [17], where v_0 is a threshold velocity related to a cutoff kinetic energy chosen arbitrarily in the range of ∼10–100 eV. The parameters β_{S_e} and $\beta_{\text{e-ph}}$ have different values, since they are considered as being originated in different physical processes. For example, the authors of Ref. [18] assume "that the e–ph coupling process is not initiated until 0.3 ps after the initiation of the collision process, as the lattice temperature is ill-defined before this. Until this time of the simulation only the electron stopping mechanism is active, while there is a time-frame when both the electronic stopping and e–ph interaction mechanisms are active."

As examples of this way of approaching the problem, we mention the works of Sand *et al.* on damage of W [19] using $\tau_{S_e} = m/\beta_{S_e} = 1$ ps for the electronic stopping (with m the mass of the ions) and no e-ph term; of Zarkadoula *et al.* on Fe [18], who used a value of $\tau_{S_e} = 1$ ps for stopping power and $\tau_{S_{\text{e-ph}}} = 1.54$ ps for the e-ph regime; and of Zhurkin and Kolesnikov in a study of cluster impacts on metals [20], who used $\tau_{\text{e-ph}} = 1$ ps for Ni and $\tau_{\text{e-ph}} = 1.7$ ps for Al. Caro and Victoria and Proennecke *et al.* considered $3.4 < \tau_{\text{e-ph}} < 10$ ps and $0.27 < \tau_{S_e} < 2.5$ ps for Cu [4,21]. It can be concluded that in the literature there is a diversity of values but always $\tau_{S_e} > \tau_{\text{e-ph}}$ by a factor between ∼1.5 and ∼10.

The aim of this work is to show that the electronic stopping power has a complex dependence on both the ion velocity and the local electronic density, which are both related to the local electronic density of states (LDOS). For a projectile to lose energy to target electrons two conditions are required, first that target electrons have to be where the projectile is and second that there have to filled states where electrons can be taken from

*caro@lanl.gov

and empty states they can fill in; both conditions are related to the structure of the LDOS. The projectile velocity provides an energy scale around the Fermi energy, similar to thermal energy $k_B T$, which determines what electrons participate in the nonadiabatic process. It is known that for the uniform electron gas the stopping power is linear in velocity for projectile velocities less than the Fermi velocity, $S_e = \beta v$, and that β has a complex density dependence [22,23], but for more realistic density of states the situation changes, as has recently been shown for the case of protons and He in Au [24].

Besides the velocity dependence, the reason that makes β_{S_e} and $\beta_{\text{e-ph}}$ different is the local electronic density (ρ) of the target, which an energetic particle can explore in different energy domains: a particle undergoing electronic stopping is an energetic particle that visits many regions in a solid, with different electronic density, while a particle moving in a phononlike mode, i.e., with meV of energy, visits regions close to their equilibrium lattice positions, where the electronic density of the host matrix has a minimum. By making explicit the β dependence on ρ we describe here the e-ph interaction as a special case of electronic stopping process at very low energies. By comparing the strength of the so determined e-ph coupling to fully quantum-mechanical treatments, we assess the validity of the Langevin equation to represent this nonadiabatic phenomenon. The main approximation we make is the assumption of classical motion for the ions at thermal energies, which is presumably valid for kinetic energies above the Debye temperature.

It is important to mention that this local-density dependence of the damping term representing the electronic stopping power was proposed by us years ago [4], but the high degree of empiricism in the functional form proposed for this dependence prevented it from being adopted as a standard approximation. Here we give the initial steps towards a functional form with *ab initio* type accuracy.

Additionally, within the framework of time-dependent tight-binding theory, Race *et al.* [17] reported results providing evidence that, for tight-binding molecular-dynamics simulations, the strength of the coupling depends on the electronic density at the crystalline location of the moving ion, giving support to this work in that the stopping mechanisms appearing in time-dependent electronic structure calculations could account for both S_e and e-ph interaction.

II. METHOD: NONADIABATIC CALCULATION

Using time-dependent density functional theory (TD-DFT) [25] to follow the energy transfer from (classical) ions to (quantum) electrons we analyze the ability of the proposed technique to calculate both the electronic stopping of an energetic projectile traveling along a channeling direction and the the e-ph interaction parameter for the case of a single representative vibrational mode, the Einstein oscillator. Both types of simulations were performed on a supercell with 108 Ni atoms (Γ-only sampling) on a fcc lattice with a lattice parameter of 3.52 Å. Norm-conserving pseudopotentials and an energy cutoff of 150 Ry for a plane-wave basis were used. The calculations included semicore states, were nonmagnetic, and used the adiabatic LDA exchange-correlation (XC) potential. For details on the implementation of TD-DFT in QBOX, see Ref. [26].

Previous work by Pruneda *et al.* and by others on nonadiabatic dynamics in insulators [27], and of Correa and coworkers on H in Al [28,29], proved that TD-DFT gives accurate results for S_e at high (i.e., $E \gg 1$ eV) energies. By accurate we mean in good agreement with the SRIM database, considered to be the standard reference for this property [30,31]. For one particular case studied in this work, namely, a Ni projectile into a Ni target at an energy of 1.5 MeV, SRIM reports a stopping of 148.2 eV/Å while our calculations for the center of a ⟨100⟩ channel give 42.5 eV/Å. This discrepancy can easily be removed by taking into consideration that experimental values represent averages of actual trajectories and, as discussed in Refs. [29,32], either running off-center channel simulations or random direction trajectories, bring the results into excellent agreement with SRIM.

In this work, we evaluate the electronic stopping for an atom in two different environments: (i) an energetic projectile in channeling conditions and (ii) an atom vibrating with thermal energies around its equilibrium position. We determine a scalar β for both cases, and relate it to the local density seen by the moving atom, which we assume is the main characteristic that distinguishes between the two environments. To this end we first evaluated the time evolution of the total electronic energy of a system composed of a Ni projectile traveling along the center of a ⟨100⟩ channel in the Ni fcc crystal. Details of these calculations will be published elsewhere; here we show in Fig. 1 the general aspect of these curves.

For the case of an atom vibrating with thermal energies around its equilibrium position, we aim at calculating the stopping power at much lower velocities, corresponding to energies in the meV region. We then face the time-scale limitations imposed by the computational cost of TD-DFT. We adopt then the following strategy: to determine if the sample size (number of electrons in the supercell calculations) is large enough in the sense that the small gaps appearing between the electronic eigenvalues are not affecting the results of the calculation, we propagate the projectile in a uniform electron gas, jellium, with the same parameters used to represent Ni in the DFT calculations, meaning the same XC functional, cutoff,

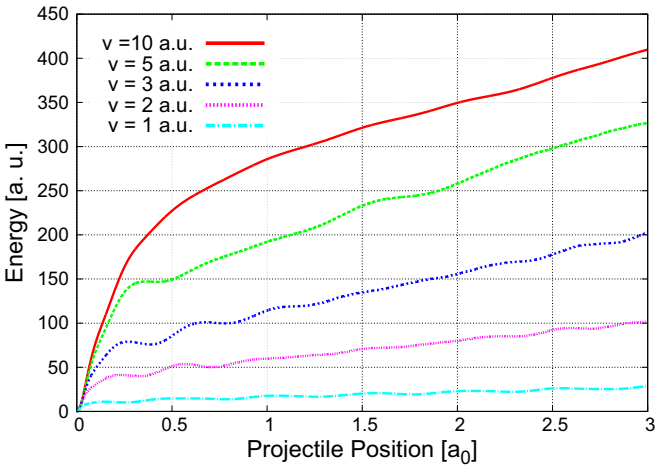

FIG. 1. (Color online) Total energy vs position of the Ni projectile across the ⟨100⟩ channel in a fcc Ni at different velocities (from 1.5 to 150 MeV). We obtained the electronic stopping power from the slope of these curves, after an initial transient.

box size, etc. The ground state of a jellium with electron density in the range we want to study (0–1.5 $e/\text{Å}^3$) is constructed with a single additional Ni atom. In the time-dependent simulation the Ni ion is then moved at constant velocity. The energy-versus-time curves show a behavior similar to that of the crystalline target, including the transient and excitation of charge oscillations that it originates, but without the periodic oscillations due to the crystalline structure [29].

Comparing the losses corresponding to Ni traveling into crystalline Ni at the center of the ⟨100⟩ channel with those of Ni traveling in jellium we conclude that, on average, Ni travels in the fcc Ni channel producing the same dissipation as if in a homogeneous medium of electronic density $\rho = 0.75\ e/\text{Å}^3$. For a velocity of 1 a.u. (1.5 MeV for Ni) the dissipation in the channel is 45 eV/Å, and β (in $S_e = \beta v$) is 2.06×10^{-3} eV ps/Å^2. This friction can be expressed in time units, as $\tau = m/\beta$, which measures the characteristic relaxation time for excess energy in the ionic system decaying into the electronic system; the relaxation time is 3.5 ps.

We use then jellium to explore the low-velocity regime because it lacks crystalline structure, which implies the need of much shorter trajectories to extract the slope representing the losses, and we can therefore determine the stopping for velocities over several orders of magnitude. Figure 2 shows S_e for a Ni projectile in jellium at a density $\rho = 1.5\ e/\text{Å}^3$ over four orders of magnitude of velocity, or equivalently eight orders of magnitude in energy, from 1.5 MeV (in the electronic stopping power regime) down to 15 meV (in the thermal phonon energy regime). The known linear dependence on the velocity is clearly confirmed (in the range of densities of interest), implying $S_e = \beta(\rho)v$. While the result shown in Fig. 2, namely, that S_e is proportional to velocity for $v < v_F$ in a uniform electron gas, is known, this figure validates the computational approach regarding sample size and emphasizes the fact that the concept of electronic stopping is valid even at thermal energies. It justifies the use of high-velocity results to study low-velocity dissipation, provided a proper treatment of the DOS at E_F for real materials is given. Going to even lower velocities in jellium should still give a linear relation, down to some limit where the discrete structure of the density of states due to the finite sample size would introduce departures from linearity, similar to those reported for insulators [27].

While jellium gives a stopping proportional to velocity, it is only an approximation to real materials and in particular to Ni, in the sense that it neglects the detailed structure of the electronic density of states (DOS) close to the Fermi energy (E_F), which translates into a velocity dependence to the coupling. We come back to this point at the Discussion section.

III. RESULTS: CONNECTION BETWEEN ELECTRONIC STOPPING POWER AND ELECTRON-PHONON COUPLING

To analyze next the connection between an energetic ion traveling along a channel and an Einstein oscillator, we study the electronic density at different locations in a Ni crystal. Figure 3 shows $\rho(x)$ along two trajectories, one along the center of a ⟨100⟩ channel, where $\rho(x)$ varies between 0.23 and 0.3 $e/\text{Å}^3$, and the other also along the ⟨100⟩ direction but across the perfect lattice sites, i.e., across the nuclei of Ni atoms. We have included in this trajectory a vacancy in the position $a_0 = 2$, to evaluate the density of Ni at a vacant site because we will picture an Einstein oscillator as a "projectile" moving around a vacant site. The figure also displays as vertical shadowed areas the size of the atom cores as given by the cutoff radius of the pseudopotential for $2p$ electrons.

Two conclusions emerge from Fig. 3. One is that the density at the center of the channel (∼0.23–0.30 $e/\text{Å}^3$), is similar but smaller than the equivalent jellium density giving the same stopping, $\rho = 0.75\ e/\text{Å}^3$ as discussed earlier. It implies that for a nonhomogeneous system, such as a crystal lattice, not only the density at the location of the nucleus of the projectile

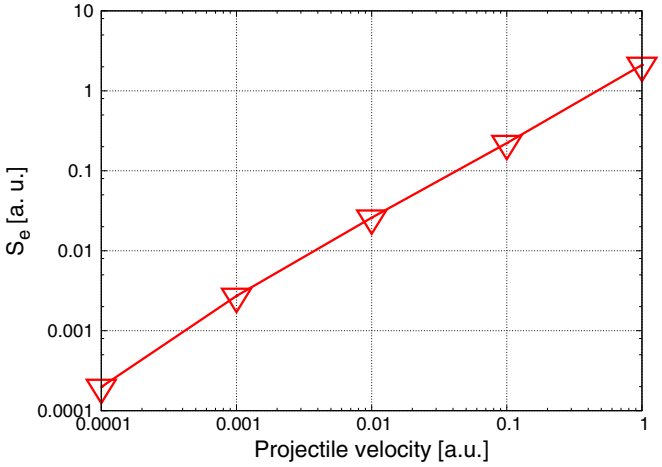

FIG. 2. (Color online) Electronic stopping S_e corresponding to Ni in jellium at metallic electron densities ($\rho = 1.5\ e/\text{Å}^3$) for different velocities covering eight orders of magnitude in kinetic energy, from 1.5 MeV (in the electronic stopping power regime) to 15 meV (corresponding to typical thermal phonon energies). The slope 1 indicates a stopping linearly proportional to velocity.

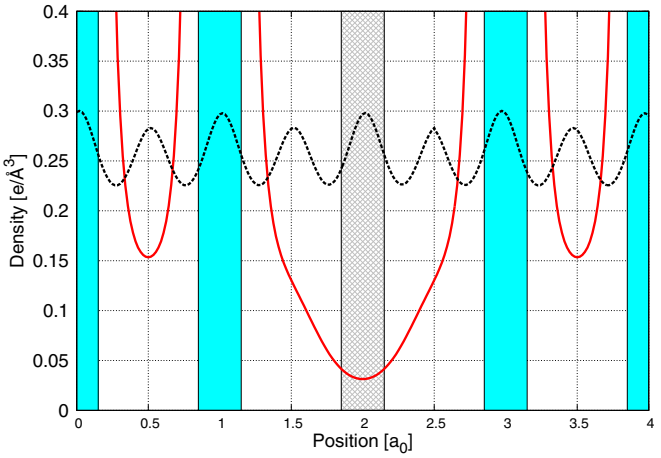

FIG. 3. (Color online) Electronic density in a fcc Ni target along two directions, the ⟨100⟩ channeling direction at its center, and along a ⟨100⟩ direction going across four atoms at positions zero, one, three, and four a_0, with a_0 the lattice parameter, and a vacancy at position $2a_0$. Note the factor of almost 10 between electronic density in the channel and at the vacant site.

is relevant, but also the density around that position. That is, the finite size of the projectile atom with its bound electrons samples regions of the target around its trajectory in a way that on average crystalline Ni stops a Ni ion traveling along the center of the channel as homogeneous jellium at $\sim 0.75\ e/\text{Å}^3$ density does. The second conclusion is that at a vacant site the electronic density is approximately ten times smaller than at the center of a channel. This fact, together with the order-of-magnitude difference in ion velocities at thermal energies, is precisely what will give rise to a different stopping for energetic projectiles than for atoms vibrating thermally around their lattice sites.

To establish the connections between S_e and e-ph interaction, we analyze now the energy dissipation of a Ni ion moving in a Ni crystal in a trajectory along a ⟨100⟩ direction passing on top of a perfect lattice site that is vacant, at two different constant velocities, namely, $v = 0.1$ and 0.05 a.u., corresponding to 15 and 3.75 keV, respectively. Phonon energies would require this study to be done at two orders of magnitude lower velocities, something that is computationally very demanding. To recover the dissipation under the real oscillatory dynamics, we will use the results for β obtained at $v = 0.05$ a.u. and plug it into the actual equation of motion of the damped harmonic oscillator at an amplitude corresponding to room temperature.

Figure 4 shows the potential energy for the BOA together with the energy according to TD-DFT for the atom moving from $x = -1.1$ to 1.1 Å, measured from the perfect crystal position where the vacancy sits, for the case $v = 0.1$ a.u. The ion in TD-DFT was set into motion at a distance from the vacancy larger than $|-1.1|$ Å, in order to reach that position well after the transient has disappeared. For visualization purposes, both curves have been vertically shifted to have equal value at $x = -1.1$ Å. Finally Fig. 4 also shows the difference between the two curves, i.e., the dissipated energy, whose

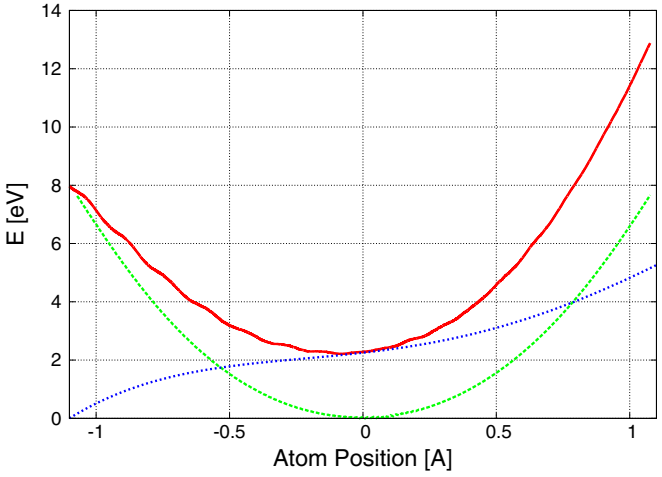

FIG. 4. (Color online) Energy vs position for an atom moving from left to right at constant velocity of $v = 0.1$ a.u. across its equilibrium position in the lattice at $x = 0$ according to both the Born-Oppenheimer approximation (dashed green curve), and nonadiabatic TD-DFT (solid-red curve). For visualization purposes, energy values have been made to coincide at $x = -1.1$ Å. The losses are given by the derivative of the curve representing the energy difference between the two approximations (dotted blue curve).

slope is the stopping power or, in this interpretation, the e-ph interaction. As it is apparent, the slope of the curve, i.e., βv, is not constant but position dependent, reflecting the fact that β is a function of the density. The curves for $v = 0.05$ a.u. are slightly different, giving a larger β.

From the curvature of the BO curve in Fig. 4 we determine the equation of motion of the Einstein oscillator by extracting Hooke's constant κ of the parabolic potential, getting $\kappa = 13.076\ \text{eV}/\text{Å}^2$. This constant determines an oscillation frequency of 7.379 THz, or a period $T_0 = 0.136$ ps. This value is to be compared with the maximum phonon frequency in Ni, which is ∼9 THz [33], reminding us that the Einstein oscillator is generally in the upper side of the phonon spectrum. From the slope of the energy difference between the adiabatic and nonadiabatic calculation reported in Fig. 4 we extract the instantaneous β as a function of position x; from the curves in Fig. 3 we obtain the density as a function of position. We can then represent β as a function of density; these functions at the two velocities considered are shown in Fig. 5. For the small variations of density considered here corresponding to displacements compatible with room-temperature excitations, the function $\beta(\rho)$ is linear in density.

This result, namely, that β is different at different velocities, clearly shows that the damping is not simply proportional to the velocity at low velocities as is the case for jellium, Fig. 2. This velocity dependence is similar to the case reported in Ref. [24] for Au. Interesting to note is the fact that the velocity dependence for Ni is just the opposite to that of Au; while in Au the coupling decreases for low velocity, in Ni it increases. The reasons for that are to be found in the structure of the DOS close to the Fermi level: while in Au increasing the width around E_F increases the number of electrons involved, in Ni it is the opposite because the Fermi level sits on a high and narrow peak. For details see Figs. 4(d) and 5(d) in Ref. [34].

The motion of a damped harmonic oscillator of mass m and damping β is exponentially attenuated with a characteristic time $\tau_A = 2m/\beta$, while the energy decays with $\tau_E = m/\beta$. We find $\tau_E = 12.7$ ps for β determined at $v = 0.1$ a.u. and $\tau_E =$

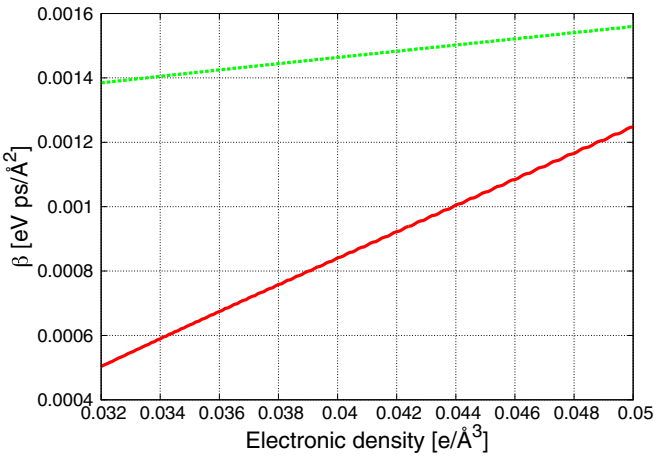

FIG. 5. (Color online) Instantaneous stopping power coefficient β vs local electronic density at the location of the projectile for a Ni atom moving along the ⟨100⟩ direction in Ni across a vacant site at 0.1 (green dashed curve) and 0.05 (red solid curve) a.u. of velocity.

4.4 ps for $v = 0.05$ a.u. We can expect that if β is calculated for lower velocities the characteristic relaxation time will be even smaller.

How does this value compare with the relaxation time for a 1.5-MeV (v = 1-a.u.) Ni particle traveling at the center of a ⟨100⟩ channel in fcc Ni? To make this comparison we will assume that for velocities between 0.1 and 1 a.u. the linear dependence of stopping with velocity is valid, which is not the case for velocities below 0.1 a.u., as we just discussed. Under this assumption, the relaxation time in a channel, namely, 3.5 ps, is 4.5 times shorter that the relaxation time around a vacancy. In terms of β for a particle traveling in a channel, $\beta(\rho = 0.25\, e/\text{Å}^3) = 2.06 \times 10^{-3}$ eV ps/Å^2, while for an atom traveling around its equilibrium position $\beta(\rho = 0.03\, e/\text{Å}^3) = 4.57 \times 10^{-4}$ eV ps/Å^2. In short, a variation of the host electronic density by a factor of ∼9 produces a variation of the strength of the coupling by a factor of ∼4.5.

This result partially solves the difficulty presented in the Introduction about the use of a piecewise function for β. However the precise relation between β and ρ at all densities, which is of relevance for practical implementations of TTM in classical MD simulations, requires also a dependence on velocity and/or on the structure of the DOS around E_F, a complex problem that still needs to be solved and is beyond the purpose of this paper.

IV. COMPARISON WITH THE PERTURBATIVE APPROACH

Finally, how does the e-ph relaxation time from TD-DFT compare with the value obtained using standard Bloch-Boltzmann-Peierls expression [35] describing the rates of change of electron and phonon distribution due to electron-phonon collision? In such approximation, the electron energy dissipation caused by the difference in electron and lattice temperatures is described by the theory developed by Allen [36]:

$$c_e \frac{dT_e}{dt} = -\pi \hbar k_B \lambda \langle \omega^2 \rangle N(E_F)(T_e - T_l) = -g(T_e - T_l) \quad (1)$$

where c_e is the electronic specific-heat capacity, $\langle \omega^2 \rangle$ is the average value of phonon frequency, $N(E_F)$ is the electronic density of states (DOS) per spin at Fermi energy, λ is the coupling constant, and T_e and T_l are electron and lattice temperatures, respectively.

The rigid muffin-tin potential approach (RMTA) proposed by Gaspari and Gyorffy [37] significantly simplifies the calculation of λ. It was used to calculate the Hopfield parameter $\eta = \lambda/(m\langle \omega^2 \rangle)$, where m is atomic mass. Thus, the zero-temperature expression for the e-ph coupling is defined as

$$g = \pi \hbar k_B \eta N(E_F)/m. \quad (2)$$

The electronic scattering phase shifts and electronic density of states, $N(E_F)$, needed to calculate η, are obtained from the atomic sphere approximation of the Korringa-Kohn-Rostoker (KKR) [38,39] calculation. Within RMTA the spherically averaged part of the Hopfield parameter is equal (in Rydberg units) to

$$\eta = 2N(E_F) \sum_\ell (\ell + 1) M^2_{\ell,\ell+1} \frac{f_\ell}{2\ell + 1} \frac{f_{\ell+1}}{2\ell + 3}, \quad (3)$$

where f_ℓ is a relative partial DOS,

$$f_\ell = \frac{N_\ell(E_F)}{N(E_F)}, \quad (4)$$

and $M_{\ell,\ell+1}$ is the electron-phonon matrix element

$$M_{\ell,\ell+1} = \int_0^S R_\ell \frac{dV}{dr} R_{\ell+1} r^2 dr, \quad (5)$$

where the gradient of the one-electron potential $V(r)$ and the radial solution of the Schrödinger equation, R_ℓ and $R_{\ell+1}$, were used. $M_{\ell,\ell+1}$ can be written [37] in terms of the phase shifts δ_ℓ or in terms of logarithmic derivatives of $D_\ell = r R'_\ell / R_\ell$ evaluated at the boundary of the atomic sphere [40–42]:

$$M_{\ell,\ell+1} = -\phi_\ell(E_F)\phi_{\ell+1}(E_F)\{[D_\ell(E_F) - \ell] \times [D_{\ell+1}(E_F) + \ell + 2] + [E_F - V(S)]S^2\}, \quad (6)$$

where $\phi_\ell(E_F)$ is the amplitude of the ℓ partial wave.

Since both η and g are proportional to $N(E_F)$, the resulting value strongly depends on the magnetic ordering in the material, namely, $\eta = 2.6$ eV/Å^2 for nonmagnetic Ni and $\eta = 2.1$ eV/Å^2 for the magnetic one. This difference is mainly caused by much higher $N(E_F)$ for nonmagnetic Ni compared to the magnetic one. The corresponding coupling values, g, are equal to 14.9×10^{17} and 9.6×10^{17} W/m^3 K. According to Lin *et al.* [34], the highest value of g, 10.5×10^{17} W/m^3 K, is measured in transient thermoreflectance experiments [43]. The electron temperature in this experiment does not exceed 100 K. The phonon relaxation is obtained using the expression $\tau_{ph} = c_l/g$, where c_l is the lattice specific-heat capacity. The resulting phonon relaxation times at temperature equal to 300 K are 3.1 ps for nonmagnetic Ni and 4.8 ps for the magnetic one, where the temperature dependence was included following the approach proposed by Wang *et al.* [44]. This approach allows us to include scattering of phonons on electrons away from the Fermi surface. Following Wang *et al.* and Lin *et al.* [34] the temperature-dependent electron-phonon coupling was calculated using

$$g(T_e) = \pi \hbar k_B \frac{\eta}{M} N(E_F) \int_{-\infty}^{\infty} dE \left[\frac{N(E)}{N(E_F)}\right]^2 \left[-\frac{\partial f}{\partial E}\right], \quad (7)$$

where $-\frac{\partial f}{\partial E}$ is the derivative of the equilibrium Fermi distribution function. At low electronic temperatures, T_e, this function reduces to a delta function, and the expression for g reduces to Eq. (2). Figure 6 shows the calculated $g(T_e)$ together with available experimental data obtained in transient thermoreflectance experiments [43] and pump-probe transmission experiments [45] and deduced from the two-temperature model for surface melting [46] (see detailed discussion in the paper by Lin *et al.* [34]). The calculated dependence is in very reasonable agreement with experiment.

V. DISCUSSION

The e-ph interaction represented in terms of a relaxation time has then been calculated with two different approaches, namely, in a semiclassical way, as the low-velocity limit of electronic stopping, producing a value for an Einstein oscillator of $\tau = 12.7$ ps for β calculated at $v = 0.1$ a.u and

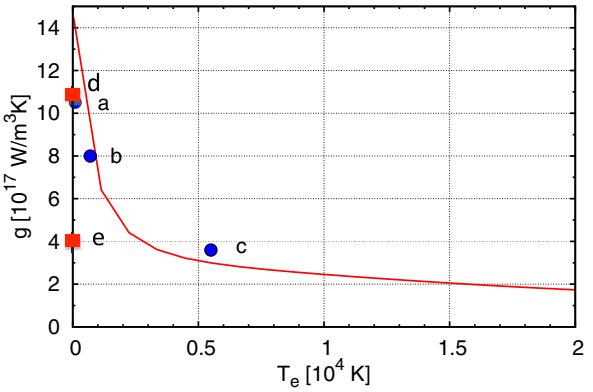

FIG. 6. (Color online) Calculated (red line) and experimental (blue dots) electron-phonon coupling as a function of electron temperature. The data point at "a" is from Ref. [43], at "b" is from Ref. [45], and at "c" is from Ref. [46]. Also shown are the points calculated as stopping power, with an instantaneous stopping power coefficient β determined with a projectile traveling at $v = 0.05$ a.u. of velocity (point d), and at $v = 0.1$ a.u. (point e). For details see text.

$\tau = 4.4$ ps for β calculated at $v = 0.05$ a.u, and as given by linear-response theory, producing a value of $\tau = 3.5$ ps at 0 K. The similarity of these results is surprising if we consider how different the two approaches are. To mention some, the e-ph interaction seen as an electronic stopping process uses Ehrenfest dynamics, which is known to misrepresent some dissipation channels [47]. Also, our calculation is for an Einstein mode, a highly localized superposition of all normal modes, while the quantum-mechanical calculation involves a thermal population of phonons. In addition, the quantum-mechanical calculation is very sensitive to the electronic DOS at the Fermi level, a usual source of numerical inaccuracy. However, the main assumption is the velocity proportionality of the stopping, as represented in Fig. 2 for jellium: the βs used for the calculation of the attenuation of an Einstein oscillator were obtained at $v = 0.1$ and 0.05 a.u., while the velocity of an atom moving in the phonon regime is in the range of $v \sim 0.0001$ a.u., implying that an even larger value of β may be found if the velocity is further reduced.

In a recent paper, Zeb *et al.* showed that, for protons on Au, where the Fermi level is in the *s* band close to the upper limit of the *d* band, the experimentally reported nonlinear behavior of stopping power versus velocity (lower slope of the stopping at lower velocities) is due to a gradual crossover as excitations tail into the *d* electron spectrum [24]. Using a similar argument for our case of Ni in Ni, we find a justification for the opposite behavior, namely, an increase in the slope of the stopping as the velocity decreases, as shown in Fig. 6. Our calculated dependence of the e-ph coupling on electronic temperature in Ni, as well as the work by Lin *et al.* [34], show a strong negative dependence in the temperature regime relevant for high-energy laser pulses, i.e., electronic temperatures up to 10^4 K. As the electronic temperature increases, electrons in a window of width $k_B T$ around E_F start to participate in the coupling and since in Ni the $N(E_F)$ is very high and decreases at both sides of E_F the coupling has a strong negative temperature dependence.

The e-ph interaction seen as a stopping process can be analyzed with the same argument, namely, the electrons that participate in the stopping are those around E_F with a width that increases with projectile velocity. Using a semiclassical argument we see that for a given projectile velocity v electrons in a range $E_F \pm 2\hbar k_F v$ become relevant for the nonadiabatic energy exchange. Therefore a meaningful comparison between electronic stopping and e-ph coupling can be made when $v \sim k_B T/(2\hbar k_F)$, with T the electronic temperature. So, for example, an electronic temperature of 5000 K corresponds, in this analogy, to a projectile velocity of 0.011 a.u. (counting ten valence electrons per nickel ion) or 0.006 a.u. (two *s* electrons per nickel ion). This argument is a good candidate to explain why the e-ph and stopping power calculations agree when both theories are compared at the appropriate limits, i.e., when both approaches effectively probe the same range of DOS around E_F.

At high electronic temperature (or in the presence of defects affecting the band structure) the exact value of $N(E_F)$ of the perfect crystal becomes less relevant, and is replaced by an average in the range $E_F \pm k_B T$. In fact, for disordered alloys, liquid phase, or high temperature, we expect that the semiclassical stopping method to the two-temperature model could become a practical and accurate approach.

VI. CONCLUSION

In summary, using TD-DFT we simulated an oscillatory ion motion with thermal energies subject to the damping created by electronic excitations, as well as an energetic ion traveling in a channel direction in a crystal. We interpreted both damping processes as being two aspects of the same physical phenomenon, differentiated only by the density of the target that the moving particle is able to explore at different energy ranges. This connection between the two processes is not new in molecular physics: Several years ago a similar assumption was made by Persson and Hellsing [48,49] to explain the attenuation of oscillating molecules or adatoms on the surface of a metal. In this paper we give a full quantitative evaluation of the process for a metal with *ab initio* accuracy. Finally, in a recent paper by Mason [50] an explicit form is given for the damping coefficient in terms of a damping tensor derived from a tight-binding model, adding more complexity to our simple scalar damping term. Still Mason's model considers S_n and S_e as distinct phenomena acting at different energy scales. Perhaps a combination of both approaches may give the most complete description on nonadiabatic phenomena in solids.

The classical trajectory is not only a technical shortcut but also makes the connection with state-of-the-art molecular-dynamics simulations. The proposition presented in this paper of calculating the e-ph interaction as a particular case of an electronic stopping process provides a simple solution to the empiricism present today in molecular-dynamics simulations of nonadiabatic processes in energetic ion-solid interactions, by attributing the differences in value of the damping coefficient β at different ion energies to the different values of the host electronic density found by moving particles when in the high-energy regime or in the thermal energy regimes. A practical implementation of this approach in a MD simulation would require an on-the-fly determination of the electronic density, obtained, for example, by superposition of spherical atomic densities (as it is currently feasible in the embedded

atom method), and a precise functional form relating β to ρ as obtained with the presented method.

ACKNOWLEDGMENTS

Work was performed at the Energy Dissipation to Defect Evolution Center, an Energy Frontier Research Center funded by the U.S. Department of Energy (Grant No. 2014ORNL1026) at Los Alamos and Oak Ridge National Laboratories. This research used resources provided by the LANL Institutional Computing Program. LANL, an affirmative action/equal opportunity employer, is operated by Los Alamos National Security, LLC, for the National Nuclear Security Administration of the U.S. Department of Energy under Contract No. DE-AC52-06NA25396. Work by A.A.C. was performed under the auspices of the U.S. Department of Energy by Lawrence Livermore National Laboratory under Contract No. DE-AC52-07NA27344.

[1] M. Born and R. Oppenheimer, Ann. Phys. (Leipzig) **389**, 457 (1927).
[2] F. Seitz and J. S. Koehler, Solid State Phys. **2**, 305 (1956).
[3] I. M. Lifshitz, M. I. Kaganov, and L. V. Tanatarov, J. Nucl. Energy **A12**, 69 (1960).
[4] A. Caro and M. Victoria, Phys. Rev. A **40**, 2287 (1989).
[5] R. Fleischer, P. Price, and R. Walker, J. Appl. Phys. **36**, 3645 (1965).
[6] D. Lesueur and A. Dunlop, Radiat. Eff. Defects Solids **126**, 163 (1993).
[7] G. Schiwietz, P. Grande, B. Skogvall, J. P. Biersack, R. Koehrbruck, K. Sommer, A. Schmoldt, P. Goppelt, I. Kadar, S. Ricz *et al.*, Phys. Rev. Lett. **69**, 628 (1992).
[8] J. Rzadkiewicz, A. Gojska, O. Rosmej, M. Polasik, and K. Slabkowska, Phys. Rev. A **82**, 012703 (2010).
[9] C. Dufour, A. Audouard, F. Beuneu, J. Dural, J. P. Girard, A. Hairie, M. Levalois, E. Paumier, and M. Toulemonde, J. Phys. Condens. Matter **5**, 4573 (1993).
[10] E. M. Bringa and R. E. Johnson, Phys. Rev. Lett. **88**, 165501 (2002).
[11] D. M. Duffy and A. M. Rutherford, J. Phys. Condens. Matter **19**, 016207 (2007).
[12] F. Gygi and G. Galli, Phys. Rev. B **65**, 220102 (2002).
[13] D. Dundas, E. McEniry, and T. Todorov, Nature Nanotech. **4**, 99 (2009).
[14] A. M. Rutherford and D. M. Duffy, J. Phys. Condens. Matter **19**, 496201 (2007).
[15] I. T. Todorov, B. Smith, K. Trachenko, and M. T. Dove, Capab. Comput. **6**, 12 (2005).
[16] I. T. Todorov, B. Smith, M. T. Dove, and K. Trachenko, J. Mater. Chem. **16**, 1911 (2006).
[17] C. P. Race, D. R. Mason, M. W. Finnis, W. M. C. Foulkes, A. P. Horsfield, and A. P. Sutton, Rep. Prog. Phys. **73**, 116501 (2010).
[18] E. Zarkadoula, S. L. Daraszewicz, D. M. Duffy, M. A. Seaton, I. T. Todorov, K. Nordlund, M. T. Dove, and K. Trachenko, J. Phys. Condens. Matter **26**, 085401 (2014).
[19] A. E. Sand, S. L. Dudarev, and K. Nordlund, Europhys. Lett. **103**, 46003 (2013).
[20] E. E. Zhurkin and A. S. Kolesnikov, Nucl. Instrum. Methods Phys. Res. B **202**, 269 (2003).
[21] S. Proennecke, A. Caro, and M. Victoria, J. Mater. Res. **6**, 483 (1990).
[22] M. J. Puska and R. M. Nieminen, Phys. Rev. B **27**, 6121 (1983).
[23] P. M. Echenique, R. M. Nieminen, and R. H. Ritchie, Solid State Commun. **37**, 779 (1981).
[24] M. A. Zeb, J. Kohanoff, D. Sánchez-Portal, A. Arnau, J. I. Juaristi, and E. Artacho, Phys. Rev. Lett. **108**, 225504 (2012).
[25] E. Runge and E. K. U. Gross, Phys. Rev. Lett. **52**, 997 (1984).
[26] A. Schleife, E. W. Draeger, Y. Kanai, and A. A. Correa, J. Chem. Phys. **137**, 22A546 (2012).
[27] J. M. Pruneda, D. Sanchez-Portal, A. Arnau, J. I. Juaristi, and E. Artacho, Phys. Rev. Lett. **99**, 235501 (2007).
[28] A. A. Correa, J. Kohanoff, E. Artacho, D. Sanchez-Portal, and A. Caro, Phys. Rev. Lett. **108**, 213201 (2012).
[29] A. Schleife, Y. Kanai, and A. A. Correa, Phys. Rev. B **91**, 014306 (2015).
[30] J. F. Ziegler, Nucl. Instr. Meth. B **219–220**, 1027 (2004).
[31] J. F. Ziegler, SRIM-2003, http://www.srim.org/SRIM/SRIMPICS/STOP02/STOP0213.gif.
[32] A. Ojanpera, A. V. Krasheninnikov, and M. Puska, Phys. Rev. B **89**, 035120 (2014).
[33] M. Kresch, O. Delaire, R. Stevens, J. Y. Y. Lin, and B. Fultz, Phys. Rev. B **75**, 104301 (2007).
[34] Z. Lin, L. Zhigilei, and V. Celli, Phys. Rev. B **77**, 075133 (2008).
[35] J. M. Ziman, *Electrons and Phonons* (Oxford University, London, 1960).
[36] P. B. Allen, Phys. Rev. Lett. **59**, 1460 (1987).
[37] G. D. Gaspari and B. L. Gyorffy, Phys. Rev. Lett. **28**, 801 (1972).
[38] J. Korringa, Physica **13**, 392 (1947).
[39] G. M. Stocks, W. M. Temmerman, and B. L. Gyorffy, Phys. Rev. Lett. **41**, 339 (1978).
[40] D. G. Pettifor, J. Phys. F **6**, 1009 (1977).
[41] D. Glötzel, D. Rainer, and H. R. Schober, Z. Phys. B **35**, 317 (1979).
[42] H. L. Skriver and I. Mertig, Phys. Rev. B **32**, 4431 (1985).
[43] A. P. Caffrey, P. E. Hopkins, J. M. Klopf, and P. M. Norris, Microscale Thermophys. Eng. **9**, 365 (2005).
[44] X. Y. Wang, D. M. Riffe, Y. S. Lee, and M. C. Downer, Phys. Rev. B **50**, 8016 (1994).
[45] E. Beaurepaire, J.-C. Merle, A. Daunois, and J.-Y. Bigot, Phys. Rev. Lett. **76**, 4250 (1996).
[46] S.-S. Wellershoff, J. Güdde, J. Hohlfeld, J. G. Müller, and E. Matthias, Proc. SPIE **3343**, 378 (1998).
[47] A. P. Horsfield *et al.*, Comp. Mat. Sci. **44**, 16 (2008).
[48] M. Persson and B. Hellsing, Phys. Rev. Lett. **49**, 662 (1982).
[49] B. Hellsing and M. Persson, Phys. Scr. **29**, 360 (1984).
[50] D. Mason, J. Phys. Condens. Matter **27**, 145401 (2015).